Impact of Distant Charge Reversals within a Robust β-Barrel Protein Pore

ARTICLE *in* THE JOURNAL OF PHYSICAL CHEMISTRY B · JULY 2010

Impact Factor: 3.3 · DOI: 10.1021/jp101311s · Source: PubMed

2 AUTHORS:

Musheer Mohammad

26 PUBLICATIONS **387** CITATIONS

SEE PROFILE

Liviu Movileanu

Syracuse University

88 PUBLICATIONS **2,202** CITATIONS

SEE PROFILE

Impact of Distant Charge Reversals within a Robust β-Barrel Protein Pore

Mohammad M. Mohammad[†] **and Liviu Movileanu***[,†,‡,§]

Department of Physics, Syracuse University, 201 Physics Building, Syracuse, New York 13244-1130, Structural Biology, Biochemistry, and Biophysics Program, Syracuse University, 111 College Place, Syracuse, New York 13244-4100, and The Syracuse Biomaterials Institute, Syracuse University, 121 Link Hall, Syracuse, New York 13244

Received: February 10, 2010; Revised Manuscript Received: May 22, 2010

Among all β-barrel pores, staphylococcal α-hemolysin (αHL), a heptameric transmembrane protein of known high-resolution crystal structure, features a high stability in planar lipid bilayers under a wide range of harsh experimental conditions. Here, we employed single-channel electrical recordings and standard protein engineering to explore the impact of two distant charge reversals within the interior of the β-barrel part of the pore. The charge reversals were replacements of lysines with aspartic acids. A charge reversal within the structurally stiff region of the β barrel near the pore constriction reduced the open-state current of the pore, but produced a quiet pore, showing current fluctuation-free channel behavior. In contrast, a charge reversal on the trans entrance, within the structurally flexible glycine-rich turn of the β barrel, increased the open-state current and produced gating activity of the pore in the form of large-amplitude and frequent current fluctuations. Remarkably, cumulative insertion of the two distant charge reversals resulted in a large-amplitude permanent blockade of the β barrel, as judged by both single-channel and macroscopic current measurements. The results from this work suggest that these distant charge reversals are energetically coupled, producing different impacts on the ionic transport, the unitary conductance and the open-state probability of the pore.

1. Introduction

β-Barrel membrane proteins, which exhibit numerous biological functions, are found in the outer membranes of mitochondria, chloroplasts, and Gram-negative bacteria.[1] These proteins show an unusually high thermostability because of the array of backbone hydrogen bonds between adjacent antiparallel β strands. For example, given that a single hydrogen bond contributes ∼0.5 kcal/mol/residue,[2] then even for a small β-strand-rich protein with 100 residues, the free energy of stabilization is ∼50 kcal/mol. There is an unprecedented interest in the exploration of structure−function relationships of β-barrel pore-forming toxins (β-PFT),[3,4] which form well-defined multimeric proteins in lipid bilayers. Among all members of the β-PFT family, the staphylococcal α-hemolysin (αHL)[5] exhibits the most robustness under various conditions of experimentation and therefore has been employed extensively in single-molecule stochastic sensing of polypeptides[6−13] and neutral polymers.[14−20]

The αHL protein forms a mushroom-shaped heptameric transmembrane (TM) pore in planar lipid bilayers (Figure 1A).[5] This protein is a highly tractable β-barrel-type pore because of the following unique combination of attributes: (i) the availability of its high-resolution structure,[5] (ii) its ease of genetic engineering,[18] (iii) its large single-channel conductance,[14] which facilitates high time-resolution single-channel electrical recordings, (iv) its high thermal stability,[21] and (v) the pore remains open indefinitely under a wide range of experimental conditions, such as pH,[22] ionic strength,[20,23] temperature,[21] transmembrane potential,[24] and osmolytes.[14,25] We hypothesized that this enhanced stability of the open-state current of the αHL protein pore can be altered severely by major electrostatic alterations of the two distant rings of attractive ion-pair interactions located on the trans and cis termini of the β barrel (Figure 1A).

The TM domain of the antiparallel β strands of αHL, protective-antigen of the anthrax toxin (PA_{63}), aerolysin, and bicomponent leukocidin (LukF−LukS) are shown in Figure 1B. The alignments of the descending (left arrow) and ascending (right arrow) strands are based upon published crystal structures, homology, or biochemical data.[5,26,27] αHL is the only TM protein pore that contains an attractive ion-pair interaction within its highly flexible glycine-rich β-barrel turn (the ion-pair residues are boxed, Figure 1B). This ion pair is formed between Lys131 and Asp127 of each of the seven subunits (Figure 1C).[5] Moreover, the αHL protein pore features a second ion-pair interaction, between Glu111 and Lys147 in each subunit of the heptamer, near the cis end of the β barrel (Figure 1C). The latter attractive ion-pair interaction is located in a much more rigid region of the β barrel.[5] In this part of the pore, the lumen narrows to form a well-defined constriction with a diameter of ∼14 Å (Figure 1A).

One way to produce major alterations in the pore electrostatics is to introduce charge reversals of the charged residues. By reversing the charge from positive to negative, a single K → D charge reversal introduces 14 negative charges within the pore lumen of the heptameric αHL protein. Moreover, a single charge reversal in each monomer (e.g., substituting Lys by Asp) induces a repulsive interaction between negatively charged side chains.

In this paper, we employed single-site mutagenesis and single-channel electrical recordings to comprehensively examine the impact of charge reversals within the pore lumen on the enhanced stability of the open-state current of the αHL pore. The charge reversals were replacements of lysines with aspartic acids. We found that a charge-reversal αHL mutation that disrupts ion-pair interactions on the cis end of the β barrel

* To whom correspondence may be addressed. Phone: (315)-443-8078. Fax: (315)-443-9103. E-mail: lmovilea@physics.syr.edu.
† Department of Physics.
‡ Structural Biology, Biochemistry, and Biophysics Program.
§ The Syracuse Biomaterials Institute.

10.1021/jp101311s
Published on Web 06/14/2010

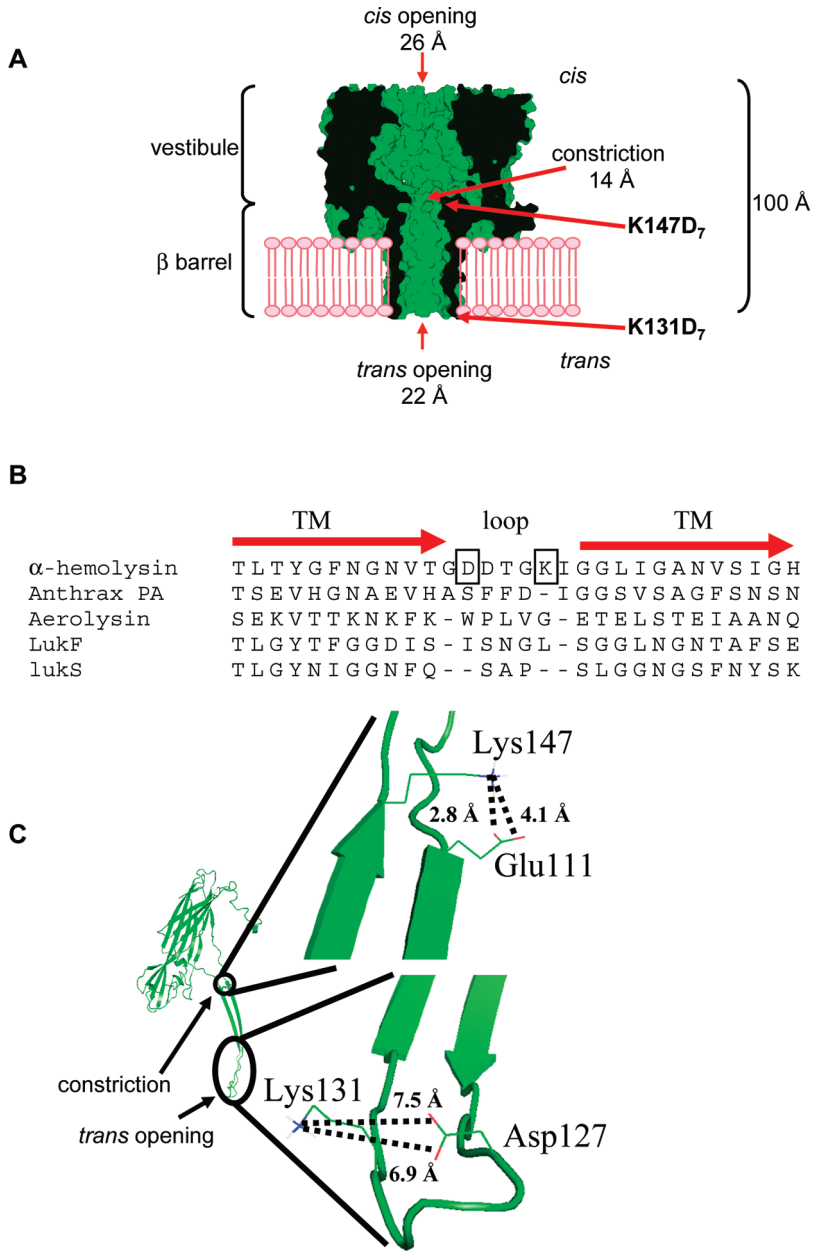

Figure 1. The distant electrostatic ion-pair interactions within the lumen of the β-barrel part of the αHL protein pore. (A) Surface of a sectional view of the αHL protein pore showing the trans opening of the pore and the constriction region. This cartoon was generated using the coordinates from the crystal structure of the αHL protein pore.[5] (B) Primary sequence alignments of the TM β strands of αHL, protective-antigen of the anthrax toxin (PA_{63}), aerolysin, and leukocidin. LukF and LukS are representatives for class F and class S of leukocidin, a bicomponent β-PFT, respectively. Amino acids involved in the long-range ion-pair interaction in the β turn of the αHL protein, D127 and K131, are boxed. (C) A single subunit showing the locations of the distant ion-pair interactions. In the restriction region, E111 forms a short-range ion-pair interaction with K147, whose N−O lengths are 4.1 and 2.8 Å, respectively. On the trans entrance of the αHL pore, which contains very short β-barrel turns, D127 forms a long-range ion-pair interaction with K131, whose N−O lengths are 7.5 and 6.9 Å, respectively.

(Figure 1A) produced a quiet single-channel electrical signature with reduced single-channel conductance. The term "quiet," which is used throughout this paper, means a protein channel that has a uniform unitary conductance and that lacks single-channel current fluctuations. In contrast, a charge-reversal αHL mutation, which disrupts an ion-pair interaction on the solvent-exposed trans end of the β barrel, produced sustained gating activity in the pore. This latter engineered αHL protein pore showed large-amplitude and frequent current fluctuations. Remarkably, the combination of the two charge-reversal αHL mutations caused the irreversible collapse of the β barrel. Collectively, our findings suggest that these major electrostatic alterations within the pore lumen of a β-barrel protein pore are energetically coupled.

2. Experimental Methods

2.1. Mutagenesis of the αHL Protein. The $K131D_7$, $K147D_7$, and $K131D_7/K147D_7$ mutants were made from the αHL gene in the plasmid that was synthetically constructed to produce unique restriction sites (αHL-RL3). Details of the construction of these mutants are published elsewhere.[28,29] Briefly, K131D and K147D were constructed by polymerase chain reaction (PCR)-based recombination as previously described.[30] K131D/K147D was constructed by cassette mutagenesis.[18] To construct the K131N/K147D mutant, α-HL-RL3 plasmid containing the K131D/K147D mutant was digested with BsiWI and StuI enzymes. The short fragment released from this digestion was synthesized except that it has the K131N mutation. This was

made by annealing two primers: 5′- GTA CGG ATT CAA CGG TAA TGT TAC TGG TGA TGA TAC AGG AAA CAT TGG AGG-3′, and 5′-CCT CCA ATG TTT CCT GTA TCA TCA CCA GTA ACA TTA CCG TTG AAT CC-3′. Thereafter, the short fragment was ligated to the aforementioned plasmid.

To generate a WT-αHL-D8 gene, we performed inverse PCR[31] on the pT-7 plasmid that contained the WT-αHL gene by utilizing the following two primers: inverse PCR primer 1: 5′-GTC ATC GTC ATC GTC ATC GTC ATC ATT TGT CAT TCC TTC-3′, and inverse PCR primer 2: 5′-**TAA** TGT AAA TTA TTT GTA CAC CAT GTA CAA ATA AAT ATA-3′. Inverse PCR primer 1 product removed the stop codon from the gene and added the DNA fragment encoding eight aspartic acid residues (those that are underlined in the primer sequence). Inverse PCR 2 primer product brought in a new stop codon (those that are in bold in the primer sequence). The unmarked sequences in inverse PCR primers 1 and 2 are part of the αHL gene and plasmid DNA, respectively. The linearized PCR product was self-ligated, and the final plasmid has the DNA code for eight aspartic acids followed by the stop codon. The insertion of the DNA code for eight aspartic acids residues was identified by DNA sequencing of the entire gene.

2.2. Expression and Purification of the Engineered αHL Protein Pores. The engineered αHL proteins were synthesized and assembled in vitro by coupled transcription and translation (IVTT) in the presence of rabbit erythrocyte cell membranes, as previously described.[17,18,21] Briefly, the [^{35}S]methionine-labeled polypeptides were purified on an 8% SDS-polyacrylamide gel. The dried gel was autoradiographed, and the bands corresponding to each αHL protein pore were excised and rehydrated in 500 μL of Milli-Q water. Gel fragments were removed with a spin filter and the resulting filtrate was stored frozen in 50 μL aliquots at −80 °C.

2.3. Electrical Recordings on Planar Lipid Bilayers. Electrical recordings were carried out with planar bilayer lipid membranes (BLMs).[32,33] The cis and trans chambers (1 mL each) of the apparatus were separated by a 25 μm-thick Teflon septum (Goodfellow Corporation, Malvern, PA). An aperture in the septum of ∼80 μm in diameter was pretreated with hexadecane (Sigma-Aldrich, St. Louis, MO) dissolved in highly purified n-heptane (Burdick and Jackson, Allied Signal Inc., Muskegon, MI) at a concentration of 10% (v/v). A 1,2 diphytanoyl-*sn*-glycero-phosphatidylcholine (Avanti Polar Lipids, Alabaster, AL) bilayer was formed across the aperture. The αHL pores were introduced by adding gel-purified homoheptamers (0.5−2.0 μL) to the cis chamber, to give a final protein concentration of 0.05−0.3 ng/mL. Single-channel currents were recorded by using a patch clamp amplifier (Axopatch 200B, Axon Instruments, Foster City, CA) connected to Ag/AgCl electrodes through agarose bridges. The cis chamber was grounded so that a positive current (upward deflection) represents positive charge moving from the trans to cis side. An Optiplex Pentium PC (Dell Computers, Austin, TX) was equipped with a DigiData 1322A A/D converter (Axon) for data acquisition. The signal was low-pass filtered with an eight-pole Bessel filter (Model 900; Frequency Devices, Ottawa, IL) at a frequency of 10 kHz and sampled at 100 kHz, unless otherwise stated. For data acquisition and analysis, we used the pClamp9.2 software package (Axon).

2.4. Determination of the Reverse Potential. To determine the ionic selectivity of the αHL protein pores, a single αHL protein pore was reconstituted into a planar lipid bilayer in symmetrical solutions of 200 mM KCl, 10 mM potassium phosphate, pH 7.4. After channel reconstitution, the cis chamber was offset to 1 M KCl, 10 mM potassium phosphate, pH 7.4. The single-channel current was then recorded versus the transmembrane potential in order to determine the reverse potential (V_r). The reverse potential, V_r, was the transmembrane potential corresponding to a zero single-channel current recorded in asymmetrical conditions.

3. Results

3.1. Charge-Reversal Mutations That Alter the Ion-Pair Interactions within the β Barrel. Many interactions might lead to αHL stability; salt bridges, hydrogen bonds, and van der Waals contacts do exist in each subunit.[5] Stabilizing or destabilizing electrostatic forces may be formed between pairs of oppositely charged residues and can result in salt bridges (′4 Å in distance, strong ion-pair interactions) and long-range interactions (>4 Å in distance, weak ion-pair interactions).[34] E111 and K147 form a strong inter- and intrasubunit ion-pair interaction within the pore lumen. E111 and K147 form ion pair interactions with N−O distances of ∼2.8 and ∼4.1 Å in the same subunit. Further, K147 of chain A forms a strong ion pair with E111 of chain B (distance d = 3.5 Å). The same situation also occurs within the flexible glycine-rich region of the pore. D127 and K131 coparticipate in long-range electrostatic interactions, with N−O distances of 7.5 and 6.9 Å in the same subunit (Figure 1C). However, a strong intersubunit ion pair interaction occurs between K131 of chain A and D128 of chain B (distance d = 3.1 Å). Taking into consideration the 7-fold symmetry of the pore complex, we conclude that there is an array of inter- and intrasubunit ion-pair interactions at the entrance and exit of the barrel.[5] Among β-PFT proteins, αHL is the only TM protein pore that contains an attractive ion-pair interaction within its highly flexible glycine-rich β-barrel turn (the ion-pair residues are boxed, Figure 1B).[5] It is worth mentioning that this region of the pore is highly exposed to solvent, so that the D127−K131 long-range electrostatic interaction is partly screened by the ions present in the aqueous phase.

We employed single-site mutagenesis combined with single-channel and macroscopic current recordings to explore the impact of two distant charge reversals of lysine residues on the enhanced open-state probability of the αHL pore. We constructed αHL protein pores where the electrostatic attractions within strategic sites of the β barrel were replaced with repulsive interactions. This was achieved by substituting the lysines in positions 131 and 147 with aspartic acids; because of the heptameric oligomerization of the αHL protein pore, the engineered αHL protein pores were denoted by K131D$_7$ and K147D$_7$ for single mutants, and K131D$_7$/K147D$_7$ for the double mutant. Therefore, the K131D$_7$/K147D$_7$ protein pore lacks all native ion-pair interactions at the cis and trans ends of the barrel.

We examined the wild-type (WT-αHL) and engineered αHL protein pores by single-channel recordings in lipid bilayers in 150 mM KCl, 10 mM phosphate buffer, pH 7.4. At a transmembrane potential of +80 mV, we observed a stable WT-αHL pore with unitary conductance of 180 ± 15 pS (n = 4 separate single-channel experiments), but decorated with infrequent (f = 0.15 ± 0.13 s^{-1}, n = 3) and very short-lived (τ = 0.73 ± 0.41 ms, n = 3) current spikes (Figure 2A). The unitary conductance is the value of the x-axis (the current amplitude) of the peak in the histogram (the right-hand panels in Figure 2). This value corresponds to the most probable state divided by the applied transmembrane potential. The dwell time and current amplitude of the current spikes were calculated with the pClamp 9.2 software (Axon) (see Experimental Methods). The average dwell time was calculated from fits with either

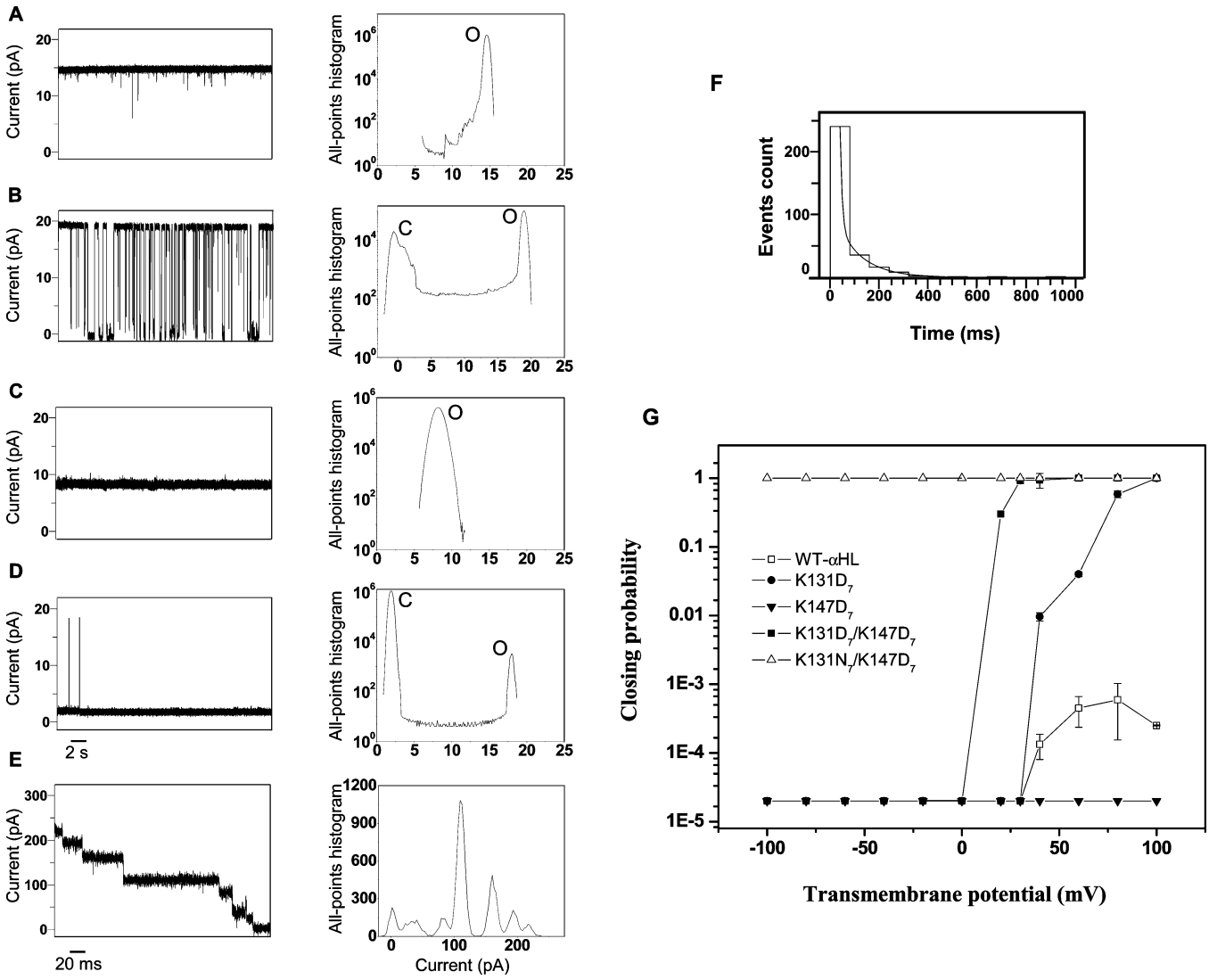

Figure 2. Representative single-channel electrical recordings of wild-type and engineered αHL proteins. (A) WT-αHL, (B) $K131D_7$, (C) $K147D_7$, (D) $K131D_7/K147D_7$, and (E) $K131N_7/K147D_7$. The applied transmembrane potential for traces in panels A−D was +80 mV. Panel E shows a multichannel current recording at a transmembrane potential of +60 mV. This panel uses a different time scale for the electrical trace because the $K131N_7/K147D_7$ pore closes very rapidly, much faster than the $K131D_7/K147D_7$ pore. Right panels: all-points amplitude histograms of the traces from A−E are presented. All single-channel current recordings were carried out in 150 mM KCl, 10 mM potassium phosphate, pH 7.4. The single-channel electrical traces were low-pass Bessel filtered at 1 kHz. O and C denote the open and closed states, respectively. (F) Representative dwell-time histogram obtained with the $K131D_7$ protein pore. The dwell-time distribution is fitted by a two-exponential curve, as determined by a log LLR test[19,35,36] with the time constants $\tau_1 = 8.9 \pm 2.9$ ms and $\tau_2 = 105.5 \pm 0.5$ ms, and the probabilities $P_1 = 0.91 \pm 0.01$ and $P_2 = 0.09 \pm 0.01$, respectively. The applied transmembrane potential was +80 mV. (G) The voltage-dependence of the closing probability of wild-type and engineered αHL protein pores. The closing probability was calculated as the time measured during the closed state divided by the total recording time. A closing probability of 1 was assigned to the αHL protein pore that did not open at a given applied transmembrane potential.

single- or double-exponential functions. The fits were judged by log likelihood ratio (LLR) tests to compare the statistical significance of different models.[19,35,36] It should be noted that the αHL protein is an open pore. Therefore, the most probable current state is the open state. In this work, the spikes are defined as brief closings not openings of the single channel. The $K131D_7$ protein pore, with an increased conductance of 240 ± 10 pS ($n = 4$), underwent current fluctuations that consisted of short-lived ($\tau_{off1} = 3.5 \pm 1.5$ ms, $n = 3$) current blockades with a frequency $f_1 = 2.8 \pm 2.0$ s^{-1} ($n = 3$), and long-lived ($\tau_{off2} = 110 \pm 40$ ms, $n = 3$) and full current blockades with a frequency $f_2 = 1.6 \pm 1.0$ s^{-1} ($n = 3$) (Figure 2B).

In contrast, the disruption of the ion pairs at E111-K147 produced a quiet $K147D_7$ pore with a decreased unitary conductance (102 ± 18 pS, $n = 5$) (Figure 2C). Moreover, a medium-sized cationic polypeptide, with a length of 23 amino acids, partitioned into the $K147D_7$ protein pore, producing short-lived current blockades (Supporting Information, Figure S1). This finding indicates that the $K147D_7$ pore is large enough to accommodate a 23 residue-long peptide into its interior. Therefore, we judge that its decreased conductance is most likely not due to protein structural changes.

3.2. Cumulative Impact of Distant Charge Reversals on the Gating Activity of the Pore. To reveal the cumulative effect of both charge-reversal mutations, we examined the $K131D_7/K147D_7$ protein pore under the same conditions as those presented above. Single-channel recordings that employed this engineered protein showed a substantially increased duration of the closed state (seconds to minutes) (Figure 2D). However, prior to complete closure of the pore, we observed current fluctuations consisting of short-lived ($\tau_{off-1} = 2.2 \pm 2.0$ ms, $n = 3$) and long-lived ($\tau_{off-2} = 1710 \pm 800$ ms, $n = 3$) current

TABLE 1: The Ionic Selectivity of the WT-αHL and Charge Reversal-Containing αHL Pores, and the Corresponding Single-Channel Conductance (g_{80}) Recorded at a Transmembrane Potential of +80 mV

pore	permeation ratio P_K/P_{Cl}	g_{80} (pS)[a]
WT-αHL	0.71 ± 0.05	180 ± 15
$K131D_7$	0.71 ± 0.12	240 ± 10
$K147D_7$	1.43 ± 0.13	102 ± 18
$K131D_7/K147D_7$	4.50 ± 0.97	225 ± 10

[a] The single-channel conductance was recorded in symmetrical buffer conditions of 150 mM KCl, 10 mM potassium phosphate, pH 7.4.

blockades with the total frequency $f = 0.20 \pm 0.12\ s^{-1}$ ($n = 3$). The unitary conductance of the $K131D_7/K147D_7$ pore was 225 ± 10 pS ($n = 3$). Notably, the corresponding electrostatic ion-pair interactions of these mutations are located far away from each other, a distance of ~49.5 Å,[5] so a significant electrostatic interaction between them is unlikely. To test whether the repulsion between the negative charges in D127, D128, and mutated D131 is the only mechanism responsible for this unusual voltage-induced gating of the engineered αHL protein pore, we also investigated the $K131N_7/K147D_7$ protein pore. We found that this engineered αHL protein pore closes even more rapidly at a transmembrane potential of +80 mV than the $K131D_7/K147D_7$ protein pore, thereby ruling out that the repulsion is the only mechanism for this unexpected rapid closure of the pore. We were able to reconstitute multichannel insertions of $K131N_7/K147D_7$, and a voltage-induced closure of multiple pores was observed in a millisecond-time scale (Figure 2E). This is the reason why the time scale of the multichannel current trace, presented in Figure 2E, is different from the time scale of the single-channel electrical traces showed in Figure 2A−D. Figure 2F shows an example of a representative dwell time histogram derived from single-channel current blockades observed with the $K131D_7$ protein pore (Figure 2B). It also shows a corresponding two-exponential curve fit, as judged by an LLR test.[19,35,36] Consistently, at transmembrane potentials lower than 100 mV, the WT-αHL, $K131D_7$, and $K131D_7/K147D_7$ protein pores exhibited voltage-induced gating activity only at positive potentials (Figure 2G). This observation is likely related to the electrostatic forces exerted on the net negative charges within the antiparallel β strands due to the applied transmembrane potential.

3.3. Cumulative Impact of Distant Charge Reversals on the Ion Selectivity of the Pore. We expected that the implementation of charge reversals on both termini of the β barrel will alter ion selectivity and ionic current rectification as well. Charge reversals, which feature multiple acidic side chains within the pore lumen, produced major changes of the pore electrostatics. Therefore, the ion selectivity of the charge reversal-containing αHL pores was modified. The permeability ratio P_K/P_{Cl} was calculated from the reverse potential (V_r) by applying the Goldman−Hodgkin−Katz (GHK) equation:[37]

$$\frac{P_K^+}{P_{Cl^-}} = \frac{[a_{Cl^-}]_t - [a_{Cl^-}]_c e^{VrF/RT}}{[a_{K^+}]_t e^{VrF/RT} - [a_{K^+}]_c} \quad (1)$$

where variable a represents the activity of either chloride or potassium in either the cis (subscript "c") or trans (subscript "t") chamber. Here, F, R, and T are the Faraday constant, gas constant, and the absolute temperature, respectively. In Table 1, we show the ionic selectivity of the WT-αHL and charge reversal-containing αHL pores, and the corresponding single-channel conductance (g_{80}) recorded at a transmembrane potential of +80 mV. Interestingly, the $K131D_7$ pore exhibited a weak anion selectivity, which was not statistically distinguished from the WT-αHL pore. One obvious interpretation is that charge reversals are located near the aqueous phase and away from the selectivity filter of the pore. In contrast, a charge reversal on the cis end of the barrel (K147D), near the pore constriction (Figure 1), altered the selectivity of the protein ($P_K/P_{Cl} = 1.43 \pm 0.13$ ($n = 3$)). Collectively, both charge reversals, on the trans and cis ends of the pore, produced a significant modification in the ion selectivity of the pore ($P_K/P_{Cl} = 4.50 \pm 0.97$ ($n = 3$)). These results demonstrate that the distant charge reversals within the pore lumen produced a nonadditive impact on both the open-state current of the pore and its ion selectivity.

3.4. The Charge Reversal-Containing αHL Protein Pores Are Heptameric. Monomers were made using IVTT and assembled into homoheptamers on rabbit red blood cell membranes (see Experimental Methods).[30,38,39] Figure 3A shows an autoradiogram of the SDS-PAGE gel, indicating the monomer and homoheptamer migration of the WT-αHL and engineered αHL protein pores relative the molecular-weight markers. To provide supplementary experimental evidence that the engineered protein pores are heptameric, we generated a mixture of WT-αHL and the mutant subunits to obtain heteroheptamer protein pores, and then we separated them on an SDS-PAGE gel. Figure 3B provides an example for the $K131D_7$ pore. The αHL protein pore and its mutants are highly SDS-stable, and therefore there should be no alteration of the gel mobility due to SDS.[21] To facilitate the separation of heteroheptameric pores on SDS-PAGE, the WT-αHL subunit was equipped with an eight aspartic acid-residue tail on the C terminus (D8) (see Experimental Methods). Heteroheptameric pores, assembled from a mixture of WT-αHL-D8 and mutant subunits, were prepared by IVTT of the WT-αHL-D8 and K131D genes together in the presence of rabbit red blood cell membranes. The resulting mixture of homoheptameric and heteroheptameric pores was separated by SDS-PAGE (Figure 3B). When the WT-αHL-D8 and K131D gene-containing plasmids were present in a ratio of 1:1, a ladder of heteroheptameric protein pores was obtained (Figure 3B).

3.5. Increasing the Salt Concentration Stabilizes the Open-State Current of the Charge Reversal-Containing αHL Protein Pores. Interestingly, single-channel electrical recordings performed with charge reversal-containing αHL protein pores, under conditions of high-salt concentrations, revealed stable open-state currents (Supporting Information, Figure S2). Even at the very low applied transmembrane potential of +20 mV, the highly unstable open-state current of the $K131D_7/K147D_7$ protein pore, observed with 150 mM KCl, is fully stabilized by raising the salt concentration at 1000 mM (Figure 4). These results suggest that the closing of charge reversal-containing αHL protein pores is governed by a complex mechanism. Presumably, an array of biophysical factors contribute to the single-molecule kinetics of channel closing, such as electro-osmotic effects, fluidity of the lipid membrane, voltage-induced undulations of the membrane and so on (Supporting Information, Figures S2−S6).

3.6. Voltage-Induced Gating of Charge Reversal-Containing αHL Protein Pores. We also examined the dependence of the single-channel current fluctuations on the applied transmembrane potential. In Figure 5, we show representative single-channel electrical recordings measured with the WT-αHL and

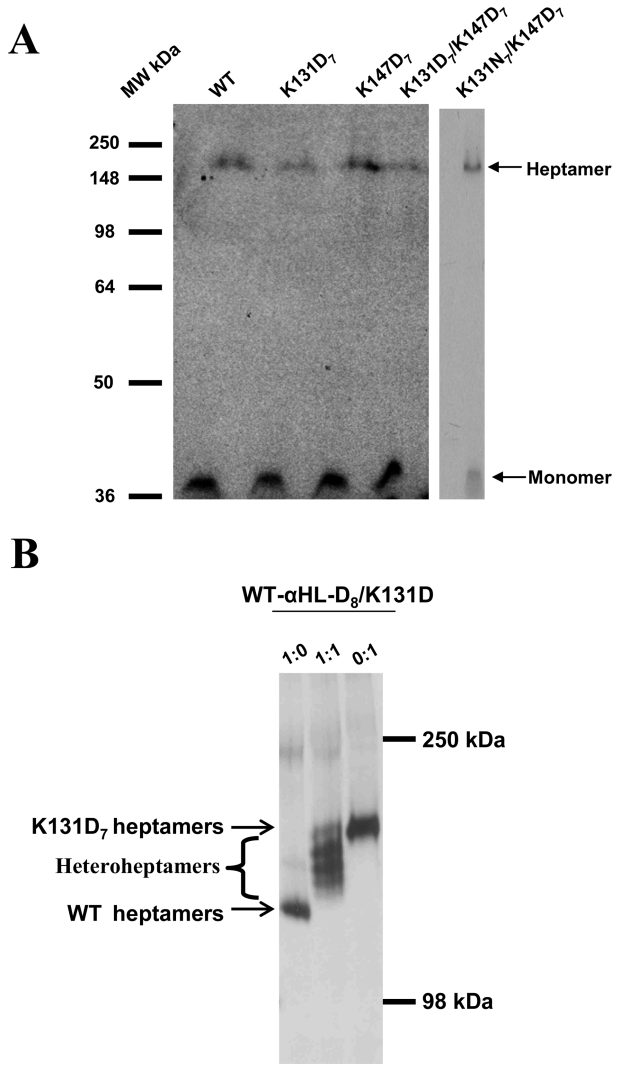

Figure 3. WT-αHL and its mutants assemble into homoheptamers. (A) Monomers were made using IVTT and assembled into homoheptamers on rabbit red blood cell membranes (see Experimental Methods).[38,39] After the translation and assembly reaction, membranes were washed with 10 mM MOPS, 15 mM NaCl, 0.1% BSA, pH 7.4 (MBSA) buffer twice and applied to 12% SDS-PAGE electrophoresis. The panel shows an autoradiogram of the SDS-PAGE gel, indicating the homoheptamer and monomer migration relative the molecular-weight markers. (B) Expression and assembly of the $K131D_7$ protein pore. WT-αHL-D8 and K131D were translated in IVTT reaction either individually or in equal ratio in the presence of red blood cell membranes.[38,39] Heteroheptamers formed by this procedure were separated on an 8% SDS-polyacrylamide gel. Molecular-weight markers are indicated on the right-hand side.

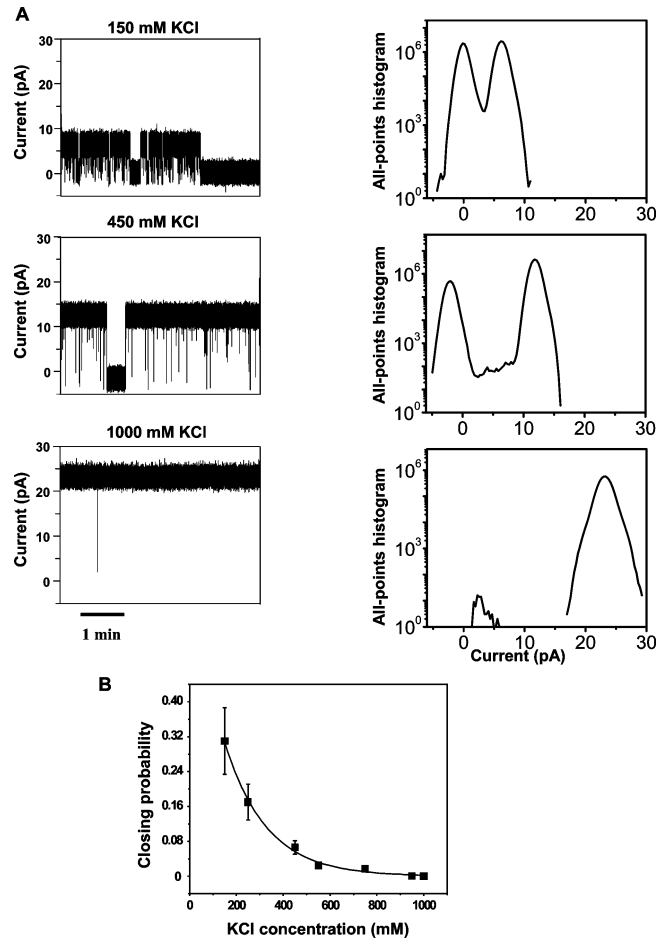

Figure 4. The $K131D_7/K147D_7$ protein pore is stabilized by the increased concentration of KCl. The buffer solution contained 10 mM potassium phosphate, pH 7.4. (A) Typical single-channel electrical traces recorded in buffer solutions containing 150, 450, and 1000 mM KCl, respectively. The single-channel electrical recordings were acquired at a transmembrane potential of +20 mV. The right-hand panels represent all-points amplitude histograms obtained for the single-channel electrical traces showed on left-side panels. (B) The dependence of the closing probability on the KCl concentration from the chamber. The closing probability was calculated as the total closing time of the pore divided by the total recording time.

charge reversal-containing αHL protein pores at applied transmembrane potentials between +20 and +100 mV. The single-channel electrical recordings were collected under symmetrical buffer solutions with both sides of the chamber containing 150 mM KCl, 10 mM potassium phosphate, pH 7.4. The WT-αHL protein pore exhibited a quiet trace at lower transmembrane potentials (less than +60 mV; Figure 5A,B). At applied transmembrane potentials greater than +60 mV, the unitary current was decorated by short-lived current spikes, the frequency of which increased with the potential (Figure 5D,E). The $K131D_7$ pore showed highly frequent, large-amplitude and short-lived current spikes even at low transmembrane potentials (<+60 mV, Figure 5B). The dependence of the frequency of the current spikes on the transmembrane potential was much sharper than that recorded with the WT-αHL protein pore. In accord with the finding presented in Figure 2C, the $K147D_7$ protein pore exhibited no gating activity (Figure 5). The $K131D_7/K147D_7$ pore exhibited long-lived current blockades, in the range of seconds, at a transmembrane potential of +20 mV (Figure 5A), whereas the channel was closed at applied transmembrane potentials greater than +60 mV (Figure 5D,E).

The sustained gating activity of the open-state current of the $K131D_7$ pore (Figure 2B) and increased close-state probability of the $K131D_7/K147D_7$ pore (Figure 2G) were not deemed to be due to improper assembly of monomers into a heptameric αHL pore prior to its insertion into the planar lipid bilayer. First, the assembly was monitored during the protein purification, and the bands that corresponded to the membrane-assembled charge-reversal αHL mutant pores were similar to those of the WT-αHL pore (Figure 3A). Second, the effect of charge-reversal mutation was voltage dependent, indicating that the closure of the channels occurs after the insertion of the fully assembled αHL pores into the bilayer (Figure 5). Third, the charge reversal-containing αHL pores reconstituted in low KCl concentration were open for long periods in high KCl concentration buffer (Figure 4), suggesting that the current blockades recorded in

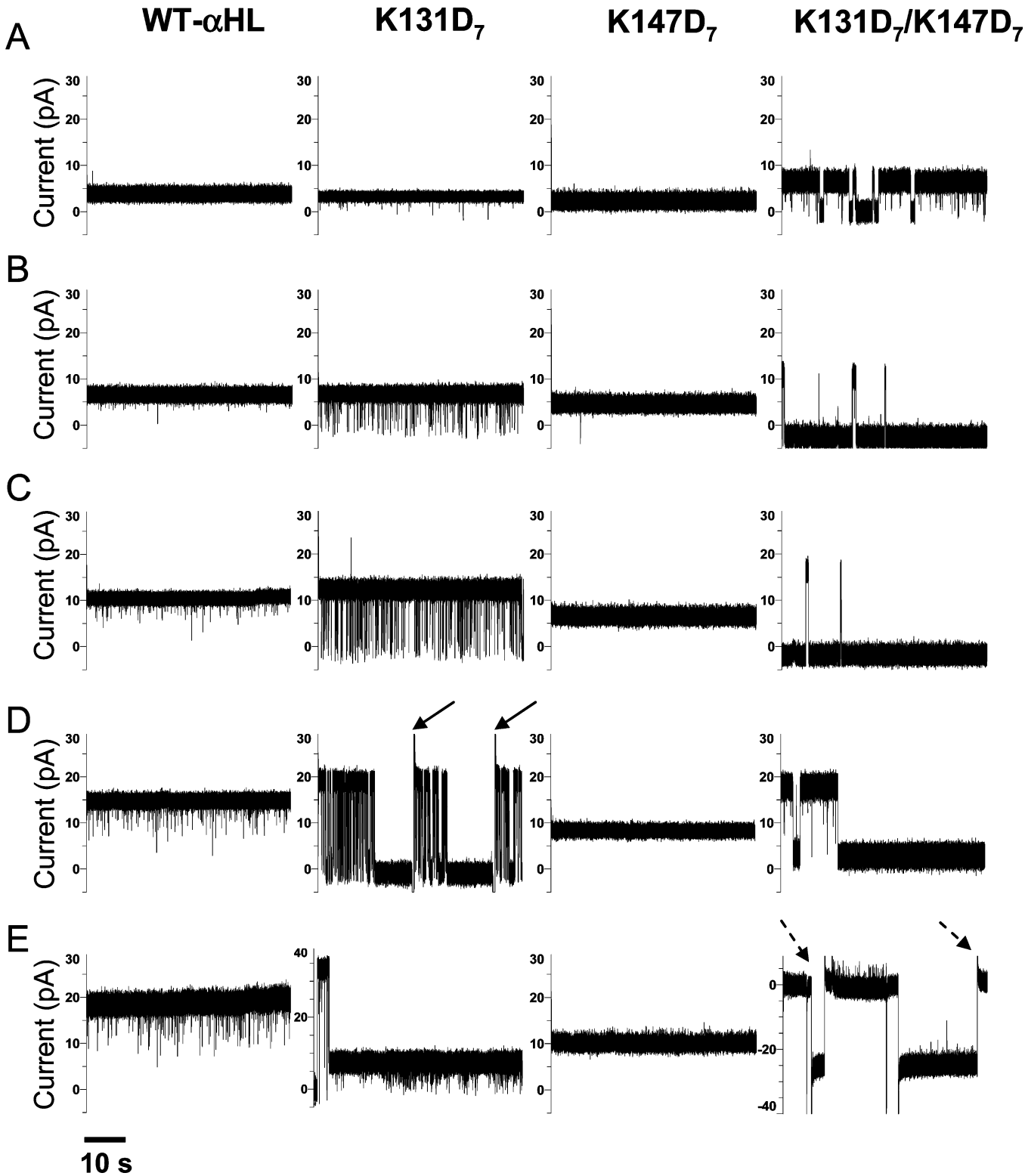

Figure 5. Representative single-channel electrical traces that show voltage-induced gating in the wild-type and engineered αHL protein pores: (A) +20 mV; (B) +40 mV; (C) +60 mV; (D) +80 mV; and (E) +100 mV. The applied transmembrane potential in the right-hand panel of E was −100 mV. In the case of the $K131D_7$ pore, the channel reopens as soon as the applied transmembrane potential is zero. The closure process is reversible. In the case of $K131D_7/K147D_7$, a transmembrane potential of −100 mV is applied to show that the channel is indeed inserted in the planar lipid bilayer. However, any application of a positive potential rapidly closes the pore for long periods. The single-channel electrical recordings were collected under symmetrical buffer solutions on both sides of the chamber containing 150 mM KCl, 10 mM potassium phosphate, pH 7.4. The single-channel electrical traces were low-pass Bessel filtered at 2 kHz. Dashed and solid arrows denote the application of positive and negative transmembrane potentials, respectively.

Figure 2 were not caused by either misfolding or improper assembly during the purification steps. The cumulative impact of distant charge reversals on the stability of the open-state current was confirmed by macroscopic (multichannel) current measurements (Figure 6). The macroscopic current traces of $K147D_7$ showed a very stable open-state current, even at a

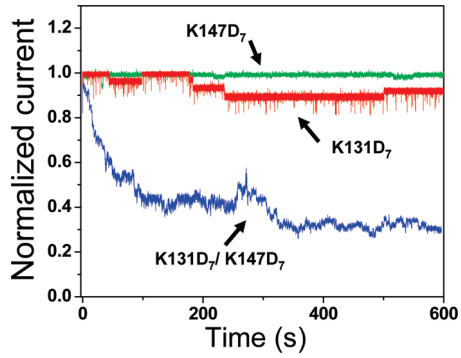

Figure 6. Macroscopic current recordings for the exploration of the instability of the open-state current of the engineered αHL protein pores. For each trace, the macroscopic current was normalized to the value that corresponded to the initial time $t = 0$. Current recordings were carried out at room temperature in 150 mM KCl, 10 mM potassium phosphate, pH 7.4. The applied transmembrane potential was +140 mV. The traces were low-pass Bessel filtered at 2 kHz.

transmembrane potential of +140 mV (Figure 6). A slow alteration of the macroscopic current was observed with the $K131D_7$ protein pore, with an apparent first-order closure rate constant of $(13 \pm 0.7) \times 10^{-4}$ s^{-1} ($n = 3$), indicating a low closing probability of this pore. In contrast, a rapid decay of the macroscopic current was recorded with the $K131D_7/K147D_7$ protein pore, with the apparent first-order closure rate constant $(13 \pm 1) \times 10^{-3}$ s^{-1} ($n = 3$), which is 1 order of magnitude faster than that value measured with the $K131D_7$ protein pore. In Figure 6, multiple, discrete macroscopic current transition states represent opening (upward transition) and closing (downward transition) of individual protein pores.

4. Discussion

The role of ion-pair interactions is not limited to protein structural stability[34,40,41] and molecular engineering;[42] they are also involved in protein−protein interactions[34] and gating activity of ion channels.[43,44] Recently, Wang and colleagues found that an ion-pair interaction plays a critical role in modulating the gating activity of the $GABA_C$ receptor.[45] Experimental evidence showed that this ion pair is broken in the open state of the channel, but stabilizes in its closed state. Voltage-induced gating is an archetype of TM β-barrel protein pores.[46] Polar interactions have a critical influence on the channel gating activity in β barrels.

Here, we employed electrophysiological data to demonstrate that the replacement of two distant ion-pair attractions by two ion-pair repulsions produces dramatic alterations in the open-state current of a robust β-barrel protein pore. Moreover, charge reversals at both termini of the β-barrel domain have an impact on the ion selectivity of the pore. Recent experimental and computational studies provided evidence that ion-pair interactions can be either stabilizing or destabilizing.[34,47] Upon the basis of the above results, we interpret that the ion-pair interactions near the trans entrance of the pore have a stabilizing effect on the open-state current. To our knowledge, the presence of an attractive ion-pair interaction at the terminal of the loop of αHL pore is unique among studied β-PFTs. For example, aerolysin features multiple attractive ion-pair interactions between lysines and glutamates on adjacent antiparallel β strands, but none of them is located on the loop terminal near the bilayer surface (Figure 1B). Why is aerolysin[48] less stable than αHL despite the numerous strong attractive ion pairs between its adjacent antiparallel β strands? We think that both the position of the ion pair and the flexibility of the β strand are key players in the stability of the open-state current of the αHL protein pore. Moreover, the αHL protein pore uniquely features an array of intersubunit ion-pair interactions, which might contribute to the unusually high stability of the open-state current. Certainly, more experimentation and computation are needed to clarify the differences in stability features between the aerolysin and αHL protein pores.

Interestingly, both the single-channel recordings and macroscopic current measurements with $K147D_7$ showed that the electrical signature is very quiet for long periods, even much longer than those current recordings obtained with the WT-αHL pore (Figure 2A,C; Figure 5). This result was surprising, because E111−K147 is a strong short-range ion-pair interaction. The K147D mutation, which introduced a net number of 14 negative charges, only reduced the unitary conductance to a lower level, likely as an effect of the alteration of pore electrostatics. Since the single-channel electrical current recorded with $K147D_7$ is stable (Figure 2C; Figure 5), we rule out that a major structural instability occurs in this mutated pore. One simple interpretation of the inability of the strong ion repulsions between E111 and D147 side chains to severely alter the open-state current of the pore is that the E111−D147 ion pair is located within the very stiff region of the β barrel.[5]

In contrast, the double charge-reversal mutation $K131D_7/K147D_7$ that disrupts both attractive ion pairs of the β barrel produces major alterations of the open-state current of the pore, as revealed by either long-lived or permanent current blockades. To our knowledge, this cumulative effect of the two distant charge reversals is unique among examined β-barrel protein pores. If the residues at positions 111−147 are not energetically coupled with those at positions 127−131, then we would expect that the changes in current fluctuations for the double mutant $K131D_7/K147D_7$ to be equal to the sum of the alterations in current fluctuations of the two single mutants $K131D_7$ and $K147D_7$. The striking effect on the open-state current observed with the double charge-reversal mutant $K131D_7/K147D_7$ is not only a result of the strong ionic repulsions resulting from the 28 negative charges (14 for each single mutant). First, the charge-reversal mutant $K147D_7$ exhibited a uniform gating-free electrical signature with a reduced unitary conductance, suggesting no major alteration of the open-state current. A double mutant $K131N_7/K147D_7$ showed a rapid current block upon the channel reconstitution at a transmembrane potential of +80 mV, indicating that the ion repulsions are not the only mechanism that might drive the channel gating observed with the $K131D_7/K147D_7$ protein pore. On the basis of our experiments with the $K131N_7/K147D_7$ protein pore, it is more than likely that the highly flexible glycine-rich loop of the β strands around D127-D131 plays a significant role in the gating activity observed with the double charge-reversal mutant $K131D_7/K147D_7$.

The results presented in this paper might stimulate future theoretical and computational studies on the dynamics of channel gating of the β-barrel protein pores. For example, full-atomistic computational efforts might be useful for estimating the single-channel current through the charge reversal-containing αHL protein pores.[49] Our expectation is that these studies will be helpful in dissecting complex biophysical phenomena and distinguishing between structural effects and the electrostatic impact on the single-channel current. In this way, the simulations would provide complementary information, in atomic detail, of the microscopic origin of the current fluctuations, which are produced by the stochastic motion of the flexible loops and turns of the β barrel.[5] Such computational work would resolve other aspects of the electrical measurements, such as the nature of

residual current under various experimental conditions, the alteration of single-channel conductance by well-designed charge-reversal mutants, as well as the impact of the alterations of the pore electrostatics on its ion selectivity.[50] Recently, an opposite behavior has been observed with an engineered αHL (7R-αHL).[51] We mention two major dissimilarities between the $K131D_7/K147D_7$ protein pores and the 7R-αHL protein pores: (i) 7R-αHL has 49 additional arginine residues engineered throughout the pore lumen, compared with the WT-αHL protein; the $K131D_7/K147D_7$ pore has two additional aspartic acid-rings (14 aspartic acids) at the entrance and the exit of the pore lumen; and (ii) 7R-αHL pores permanently close at high salt concentrations; the $K131D_7/K147D_7$ pore closes only at low salt concentrations. It is conceivable that 49 additional arginine residues impact dramatically the stability of the open-state current even at high salt concentration, contrasting the results shown in this paper. Our work also shows that strategic localizations of aspartic acid rings at the entry and exit of the pore lumen can generate distinct electrical signatures of the αHL protein.

In summary, we demonstrate that two distant charge reversals within the lumen of a β-barrel protein have a distinct impact on not only ion selectivity and unitary conductance, but also on the open-state current of the pore. Given the tractability of β-barrel pores with protein design, electrophysiological, computational, and structural examinations hold promise for the engineering of stiff protein nanopores as quiet sensor elements in stochastic single-molecule sensing. For example, the bacterial outer membrane proteins might be genetically engineered by implementing stabilizing electrostatic interactions in the extracellular loops and on both termini of the β barrel. This methodology would also be well-suited for a comprehensive exploration of the folding and stability of membrane proteins by detecting targeted regions of the β barrel that are loosely packed or tightly folded.

Acknowledgment. The authors thank Hagan Bayley and Steve Cheley (Oxford) for kindly providing the αHL-RL3 plasmids, and Ioan Andricioaei and Aaron J. Woolfe for stimulating discussions. This work was supported in part by the US National Science Foundation (HRD-0703452 and DMR-706517), the National Institutes of Health (R01 GM088403), and by the Syracuse Biomaterials Institute.

Supporting Information Available: Current blockades produced by a cationic polypeptide on the $K147D_7$ pore, the open-state current of the engineered pores at high-ionic strength concentration, the ionic selectivity of engineered αHL pores, the lack of the stability of the open-state current in low KCl concentration and at low pH, and stabilizing the open-state current of the charge-reversal αHL mutant pores by high-ionic strength buffer. This material is available free of charge via the Internet at http://pubs.acs.org.

Abbreviations

αHL	α-hemolysin protein
a	Ionic activity
β-PFT	β-barrel pore-forming toxins
BLM	Bilayer lipid membrane
g	Single-channel ionic conductance
GHK	The Goldman−Hodgkin−Katz equation
IVTT	In vitro by coupled transcription and translation
LLR	Log likelihood ratio test
LukF−LukS	Bicomponent leukocidin protein
OmpA	Outer membrane protein A
PA_{63}	Protective antigen of the anthrax toxin
P_{Cl}/P_K	Permeability ratio of chloride versus potassium
SDS-PAGE	Sodium-dodecylsulphate-polyacrylamide gel electrophoresis
TM	Transmembrane domain
V_r	Reverse potential
WT-αHL	The wild-type α-hemolysin protein pore

References and Notes

(1) Paschen, S. A.; Neupert, W.; Rapaport, D. Biogenesis of β-barrel membrane proteins of mitochondria. *Trends Biochem. Sci.* **2005**, *30* (10), 575–582.

(2) Cantor, C. R.; Schimmel, P. R. *Biophysical Chemistry - Part I: The Conformation of Biological Macromolecules*; W. H. Freeman and Company: New York, 1980.

(3) Tilley, S. J.; Saibil, H. R. The mechanism of pore formation by bacterial toxins. *Curr. Opin. Struct. Biol.* **2006**, *16* (2), 230–236.

(4) Gonzalez, M. R.; Bischofberger, M.; Pernot, L.; van der Goot, F. G.; Freche, B. Bacterial pore-forming toxins: The (w)hole story. *Cell. Mol. Life Sci.* **2008**, *65* (3), 493–507.

(5) Song, L. Z.; Hobaugh, M. R.; Shustak, C.; Cheley, S.; Bayley, H.; Gouaux, J. E. Structure of staphylococcal α-hemolysin, a heptameric transmembrane pore. *Science* **1996**, *274* (5294), 1859–1866.

(6) Goodrich, C. P.; Kirmizialtin, S.; Huyghues-Despointes, B. M.; Zhu, A. P.; Scholtz, J. M.; Makarov, D. E.; Movileanu, L. Single-molecule electrophoresis of β-hairpin peptides by electrical recordings and Langevin dynamics simulations. *J. Phys. Chem. B* **2007**, *111* (13), 3332–3335.

(7) Oukhaled, G.; Mathe, J.; Biance, A.-L.; Bacri, L.; Betton, J.-M.; Lairez, D.; Pelta, J.; Auvray, L. Unfolding of proteins and long transient conformations detected by single nanopore recording. *Phys. Rev. Lett.* **2007**, *98* (15), 158101.

(8) Stefureac, R.; Waldner, L.; Howard, P.; Lee, J. S. Nanopore analysis of a small 86-residue protein. *Small* **2008**, *4* (1), 59–63.

(9) Stefureac, R. I.; Lee, J. S. Nanopore analysis of the folding of zinc fingers. *Small* **2008**, *4* (10), 1646–1650.

(10) Movileanu, L. Squeezing a single polypeptide through a nanopore. *Soft Matter* **2008**, *4* (5), 925–931.

(11) Mohammad, M. M.; Prakash, S.; Matouschek, A.; Movileanu, L. Controlling a single protein in a nanopore through electrostatic traps. *J. Am. Chem. Soc.* **2008**, *130* (12), 4081–4088.

(12) Movileanu, L. Interrogating single proteins through nanopores: Challenges and opportunities. *Trends Biotechnol.* **2009**, *27* (6), 333–341.

(13) Madampage, C. A.; Andrievskaia, O.; Lee, J. S. Nanopore detection of antibody prion interactions. *Anal. Biochem.* **2010**, *396* (1), 36–41.

(14) Bezrukov, S. M.; Vodyanoy, I.; Brutyan, R. A.; Kasianowicz, J. J. Dynamics and free energy of polymers partitioning into a nanoscale pore. *Macromolecules* **1996**, *29* (26), 8517–8522.

(15) Bezrukov, S. M. Ion channels as molecular Coulter counters to probe metabolite transport. *J. Membr. Biol.* **2000**, *174* (1), 1–13.

(16) Bezrukov, S. M.; Kasianowicz, J. J. Neutral polymers in the nanopores of alamethicin and α-hemolysin. *Biol. Membr.* **2001**, *18* (6), 453–457.

(17) Movileanu, L.; Bayley, H. Partitioning of a polymer into a nanoscopic protein pore obeys a simple scaling law. *Proc. Natl. Acad. Sci. U.S.A.* **2001**, *98* (18), 10137–10141.

(18) Movileanu, L.; Cheley, S.; Howorka, S.; Braha, O.; Bayley, H. Location of a constriction in the lumen of a transmembrane pore by targeted covalent attachment of polymer molecules. *J. Gen. Physiol.* **2001**, *117* (3), 239–251.

(19) Movileanu, L.; Cheley, S.; Bayley, H. Partitioning of individual flexible polymers into a nanoscopic protein pore. *Biophys. J.* **2003**, *85* (2), 897–910.

(20) Rodrigues, C. G.; Machado, D. C.; Chevtchenko, S. F.; Krasilnikov, O. V. Mechanism of KCl enhancement in detection of nonionic polymers by nanopore sensors. *Biophys. J.* **2008**, *95* (11), 5186–5192.

(21) Jung, Y.; Bayley, H.; Movileanu, L. Temperature-responsive protein pores. *J. Am. Chem. Soc.* **2006**, *128* (47), 15332–15340.

(22) Bezrukov, S. M.; Kasianowicz, J. J. Current noise reveals protonation kinetics and number of ionizable sites in an open protein ion channel. *Phys. Rev. Lett.* **1993**, *70* (15), 2352–2355.

(23) Krasilnikov, O. V.; Rodrigues, C. G.; Bezrukov, S. M. Single polymer molecules in a protein nanopore in the limit of a strong polymer−pore attraction. *Phys. Rev. Lett.* **2006**, *97* (1), 018301.

(24) Movileanu, L.; Schmittschmitt, J. P.; Scholtz, J. M.; Bayley, H. Interactions of the peptides with a protein pore. *Biophys. J.* **2005**, *89* (2), 1030–1045.

(25) Krasilnikov, O. V.; Bezrukov, S. M. Polymer partitioning from nonideal solutions into protein voids. *Macromolecules* **2004**, *37* (7), 2650–2657.

(26) Miles, G.; Movileanu, L.; Bayley, H. Subunit composition of a bicomponent toxin: Staphylococcal leukocidin forms an octameric transmembrane pore. *Protein Sci.* **2002**, *11* (4), 894–902.

(27) Iacovache, I.; Paumard, P.; Scheib, H.; Lesieur, C.; Sakai, N.; Matile, S.; Parker, M. W.; van der Goot, F. G. A rivet model for channel formation by aerolysin-like pore-forming toxins. *EMBO J.* **2006**, *25* (3), 457–466.

(28) Wolfe, A. J.; Mohammad, M. M.; Cheley, S.; Bayley, H.; Movileanu, L. Catalyzing the translocation of polypeptides through attractive interactions. *J. Am. Chem. Soc.* **2007**, *129* (45), 14034–14041.

(29) Mohammad, M. M.; Movileanu, L. Excursion of a single polypeptide into a protein pore: Simple physics, but complicated biology. *Eur. Biophys. J.* **2008**, *37* (6), 913–925.

(30) Movileanu, L.; Howorka, S.; Braha, O.; Bayley, H. Detecting protein analytes that modulate transmembrane movement of a polymer chain within a single protein pore. *Nat. Biotechnol.* **2000**, *18* (10), 1091–1095.

(31) Akiyama, K.; Watanabe, H.; Tsukada, S.; Sasai, H. A novel method for constructing gene-targeting vectors. *Nucleic Acids Res.* **2000**, *28* (16), E77.

(32) Movileanu, L.; Neagoe, I.; Flonta, M. L. Interaction of the antioxidant flavonoid quercetin with planar lipid bilayers. *Int. J. Pharm.* **2000**, *205* (1−2), 135–146.

(33) Biswas, S.; Mohammad, M. M.; Movileanu, L.; van den Berg, B. Crystal structure of the outer membrane protein OpdK from *Pseudomonas aeruginosa*. *Structure* **2008**, *16* (7), 1027–1035.

(34) Kumar, S.; Nussinov, R. Close-range electrostatic interactions in proteins. *ChemBioChem* **2002**, *3* (7), 604–617.

(35) McManus, O. B.; Blatz, A. L.; Magleby, K. L. Sampling, log binning, fitting, and plotting durations of open and shut intervals from single channels and the effects of noise. *Pflugers Arch.* **1987**, *410* (4−5), 530–553.

(36) McManus, O. B.; Magleby, K. L. Kinetic states and modes of single large-conductance calcium-activated potassium channels in cultured rat skeletal-muscle. *J. Physiol. (London)* **1988**, *402*, 79–120.

(37) Hille, B. *Ion Channels of Excitable Membranes*, 3rd ed; Sinauer Associates, Inc.: Sunderland, MA, 2001.

(38) Howorka, S.; Movileanu, L.; Lu, X. F.; Magnon, M.; Cheley, S.; Braha, O.; Bayley, H. A protein pore with a single polymer chain tethered within the lumen. *J. Am. Chem. Soc.* **2000**, *122* (11), 2411–2416.

(39) Howorka, S.; Movileanu, L.; Braha, O.; Bayley, H. Kinetics of duplex formation for individual DNA strands within a single protein nanopore. *Proc. Natl. Acad. Sci. U.S.A.* **2001**, *98* (23), 12996–13001.

(40) Takahashi, T. Significant role of electrostatic interactions for stabilization of protein assemblies. *Adv. Biophys.* **1997**, *34*, 41–54.

(41) Bosshard, H. R.; Marti, D. N.; Jelesarov, I. Protein stabilization by salt bridges: Concepts, experimental approaches and clarification of some misunderstandings. *J. Mol. Recognit.* **2004**, *17* (1), 1–16.

(42) Sindelar, C. V.; Hendsch, Z. S.; Tidor, B. Effects of salt bridges on protein structure and design. *Protein Sci.* **1998**, *7* (9), 1898–1914.

(43) Liu, N.; Delcour, A. H. The spontaneous gating activity of OmpC porin is affected by mutations of a putative hydrogen bond network or of a salt bridge between the L3 loop and the barrel. *Protein Eng.* **1998**, *11* (9), 797–802.

(44) Cui, G.; Zhang, Z. R.; O'Brien, A. R.; Song, B.; McCarty, N. A. Mutations at arginine 352 alter the pore architecture of CFTR. *J. Membr. Biol.* **2008**, *222* (2), 91–106.

(45) Wang, J.; Lester, H. A.; Dougherty, D. A. Establishing an ion pair interaction in the homomeric rho1 γ-aminobutyric acid type A receptor that contributes to the gating pathway. *J. Biol. Chem.* **2007**, *282* (36), 26210–26216.

(46) Bainbridge, G.; Gokce, I.; Lakey, J. H. Voltage gating is a fundamental feature of porin and toxin β-barrel membrane channels. *FEBS Lett.* **1998**, *431* (3), 305–308.

(47) Xiao, L.; Honig, B. Electrostatic contributions to the stability of hyperthermophilic proteins. *J. Mol. Biol.* **1999**, *289* (5), 1435–1444.

(48) Chakraborty, T.; Schmid, A.; Notermans, S.; Benz, R. Aerolysin of *Aeromonas sobria*: Evidence for formation of ion-permeable channels and comparison with α-toxin of *Staphylococcus aureus*. *Infect. Immun.* **1990**, *58* (7), 2127–2132.

(49) Aksimentiev, A.; Schulten, K. Imaging α-hemolysin with molecular dynamics: Ionic conductance, osmotic permeability, and the electrostatic potential map. *Biophys. J.* **2005**, *88* (6), 3745–3761.

(50) Merzlyak, P. G.; Capistrano, M. F.; Valeva, A.; Kasianowicz, J. J.; Krasilnikov, O. V. Conductance and ion selectivity of a mesoscopic protein nanopore probed with cysteine scanning mutagenesis. *Biophys. J.* **2005**, *89* (5), 3059–3070.

(51) Maglia, G.; Heron, A. J.; Hwang, W. L.; Holden, M. A.; Mikhailova, E.; Li, Q.; Cheley, S.; Bayley, H. Droplet networks with incorporated protein diodes show collective properties. *Nat. Nanotechnol.* **2009**, *4* (7), 437–440.

JP101311S